method established that $Me_3SiOSiMe_3$ is more basic than $HMe_2SiOSiMe_2H$) so a detailed comparison is not possible. The technique here gives a measure of (Bronsted) basicity by comparing the relative stabilization of protonated ion-paired species and differentiates between linear, branched, and cyclic siloxanes, whereas the hydrogen-bonding studies provided insight into the (Lewis[23]) basicity differences between siloxanes, alkoxysilanes, and ethers. The order of basicity established in this paper (linear siloxanes > dialkyl ether > branched siloxanes > cyclic siloxanes) can be explained by inductive effects alone and was shown to be medium dependent; the interpretation of hydrogen-bonding results (basicity order: ethers > alkoxysilanes ≫ siloxanes) invoked delocalization of oxygen lone pair electrons;[24] the explanation of proton-affinity data combined lone pair delocalization with polarization of the total electron distribution by the strong acid. All of the techniques and interpretations are valid—there is no one single measure of basicity.

Experimental Section

The siloxanes in this study are commercially available (Petrarch Systems). Benzene and acetonitrile (both Aldrich spectrophotometric grade) and the substrates were distilled (with reduced pressure where appropriate) under nitrogen from CaH_2, then degassed, and stored under N_2. Hexamethylcyclotrisiloxane in benzene was stirred with CaH_2, and then the solvent was removed under vacuum followed by sublimation. The 4-chloro-2-nitroaniline (λ_{max} = 404 nm, ϵ = 4900 M^{-1} cm^{-1}) and 2-nitroaniline (λ_{max} = 391 nm, ϵ = 5300 M^{-1} cm^{-1}) reference bases were recrystallized from dry benzene. Trifluoromethanesulfonic acid (Aldrich) was used as received in ampules that were opened in a drybox (Vacuum Atmospheres) equipped with a HE-493 Dri-Train and maintained under a positive pressure of nitrogen. Glassware was oven-dried (240 °C) and then cooled under vacuum either on a double manifold or in the antechamber of the drybox. All solutions were prepared in the drybox. The integrity of test solutions was monitored by gas chromatography (Hewlett-Packard 5890A equipped with a 30 m × 0.32 mm × 0.25 μm film thickness DB5 column (J & W Scientific) and flame ionization detector).

The reference base and substrates were accurately weighed (at least 1.000 g) into dry Schlenk-type volumetric flasks on an analytical balance outside of the drybox and then frozen in liquid N_2, degassed, thawed, taken into the drybox, and diluted appropriately to give 10^{-3} M stock solutions. Concentrations of triflic acid stock solutions (prepared fresh daily) were determined by titration with standard KOH in MeOH (Aldrich) with use of tetrabromophenolphthalein ethyl ester (Eastman Kodak) as the indicator in toluene/isopropyl alcohol. Aliquots from the substrate, reference base, and acid stock solutions were transferred by pipet (at least 3 mL) to a 25-mL volumetric flask and diluted, resulting in a test solution that was 6×10^{-4} M in substrate and 3×10^{-4} M in reference base and acid. Spectroscopic cells were of a no-air design. A temperature-regulated rectangular cell holder (Perkin-Elmer 570-0705) with a digital controller (Perkin-Elmer 570-0701) was calibrated with a type K thermocouple. The test solutions were maintained at a particular temperature for about 10 min to achieve temperature equilibration and signal stability before data acquisition. Spectra were acquired on a Shimadzu UV-240 spectrophotometer at 20, 30, 40, 50, and 60 °C. The variable-temperature behavior was reproducible with each particular solution. The absorbance of the test solutions increased 77–309% between 20 and 60 °C, depending on the substrate. All absorbance readings were in the range 0.14–1.56.

The equilibrium constant was calculated at each temperature from the absorbance measurement (free RB) and the total amounts of RB, S, and HA. The treatment was simplified by the use of concentrations rather than activities. A linear least-squares fit of ln K_{eq} vs $1/T$ (all $R^2 \geq 0.95$) allowed determination of ΔH and ΔS and then calculation of ΔG(300 K) and K_{eq}(300 K). Three data sets were analyzed for each substrate and average values ± 1 standard deviation are reported in Table I.

Acknowledgment. I thank Dr. Kennith Smith for encouragement and many helpful discussions and Drs. Gregory Gillette, Joseph King, and Jonathan Rich for critical reading of the manuscript.

(23) West, R.; Baney, R. H.; Powell, D. L. *J. Am. Chem. Soc.* **1960**, *82*, 6269–6272.
(24) More recent explanations consider the detailed nature of the highest occupied molecular orbitals: Shambayati, S.; Blake, J. F.; Wierschke, S. G.; Jorgensen, W. L.; Schreiber, S. L. *J. Am. Chem. Soc.* **1990**, *112*, 697–703.

Interfacial Behavior of Block Polyelectrolytes. 1. Evidence for Novel Surface Micelle Formation†

Jiayi Zhu, Adi Eisenberg,* and R. Bruce Lennox*

Contribution from the Department of Chemistry, McGill University, 801 Sherbrooke Street West, Montreal, Quebec, H3A 2K6 Canada. *Received October 25, 1990*

Abstract: Monolayers of a polystyrene/poly-4-vinylpyridine AB diblock ionomer, $(PS)_{260}$ $(4\text{-}PVP)_{240}$, fully quaternized with decyl iodide have been studied at the air/water interface with the Langmuir film balance technique. Surface pressure/area isotherms exhibit an abrupt onset and an apparent first-order phase transition at high pressures. Transmission electron micrographs of LB films deposited on carbon-coated copper grids provide direct evidence of self-assembly of the diblock copolymers into circular surface micelles. These surface micelles appear to be quite regular and have an aggregation number of ~120. The distance between micelles (at low surface pressures) is consistent with fully extended dec-4-PVP^+ chains extending radially from a central core of PS coils. These aggregates pack with a surface density ~10^{10} particles per cm^2 at the lowest detectable surface pressures. The apparent first-order phase transition correlates with transmission electron micrograph observations and may originate from a process where the decylated polyelectrolyte block proceeds from a surface-adsorbed state to a submerged, aqueous state as the film is compressed. The entropy of this transition is +7.6 eu and is consistent with the polymeric micelles passing from an ordered 2D state to a less ordered quasi-2D state.

Introduction

Polymer monolayers, spread at the air–water interface, have played an important role in our understanding of the factors controlling polymer–polymer and polymer–interface interactions.[1-3] Details concerning molecular orientations, monomer conformations, and interaction energies are in principle determinable with the surface film balance technique[4] and ancillary spectroscopic

* Authors to whom correspondence may be sent.
† Presented in part at the 33rd IUPAC International Symposium on Macromolecules (Section 2.9.4); Montreal, July 1990.

(1) Crisp, D. J. In *Surface Phenomena in Chemistry and Biology*; Danielli, J. F., Parkhurst, K. G. A., Riddiford, A. C., Eds.; Pergamon: London, 1958.
(2) Plaisance, M.; Ter-Minassian-Saraga, L. *J. Colloid Interface Sci.* **1976**, *56*, 33.
(3) (a) Tredgold, R. H. *Thin Solid Films* **1987**, *152*, 223. (b) Malcolm, B. R. *Proc. Roy. Soc. A* **1968**, 305, 363.

0002-7863/91/1513-5583$02.50/0

methods.[5-7] In terms of polymer systems, the distribution of amino acids in proteins and monomers in random copolymers reduces the level of interpretation considerably. For this reason we are interested in measuring, as have been several groups before us,[8-12] the interfacial properties of block copolymers. Highly monodisperse segregated block copolymers with ionic segments (AB) possess the gross features of small molecular weight amphiphiles (fatty acids, phospholipids, etc.) which form well-characterized stable self-assembled structures such as micelles and bilayer vesicles and have considerable interfacial activity. Triblock copolymers (ABA) in fact are structurally related to a fascinating, relatively recently studied class of amphiphiles called boloforms.[13]

In several previous film balance studies of AB block copolymers,[8-12] a hydrophobic block (PMMA, polymethylmethacrylate; PS, polystyrene) has been linked to a hydrophilic block (PEO, polyethylene oxide; PAA, polyacrylic acid; Et-PVP$^+$, ethylated polyvinylpyridine), and the relative contributions made by the hydrophobic "buoy" block and the water soluble polyelectrolyte/polyhydrophile block have been addressed. In this paper we report the air–water interfacial behavior of an AB diblock where A = PS and B = decylated PVP$^+$. The alkylation of the short vinylpyridine block with a long chain leads to a material in the solid state which was recently descriptively termed a "bottlebrush" ionomer.[14] An unusual temperature dependence in the surface pressure-area isotherms, small onset areas, and transmission electron micrographs of Langmuir–Blodgett monolayer films suggests that these AB diblock/comb copolymers self-assemble at very low surface concentrations into quite regular 2D surface micelles. Evidence is presented that shows that these surface micelles rearrange at high surface concentration and high film pressures to form a quasi-2D thin film at the surface.

It should be recalled that the normal solution behavior of block copolymer micelles or aggregates has been studied in detail.[15] This behavior has been studied also for block copolymers containing ionic segments.[14,16] In the solid state, many block copolymers are known to be phase separated, and the morphology of these systems has been the subject of extensive studies.[17] Block ionomers have also been explored in this connection.[14,18,19] All these systems phase separate or aggregate in the solid state because of the existence of a thermodynamic driving force for phase separation. What makes the block ionomers unique is the very large value of this driving force and our ability to control that value over wide ranges by regulating the hydrophilic/hydrophobic balance through a variation of the molecular parameters of the two blocks.

Experimental Section

Polymer Synthesis and Characterization. The AB block poly(S-b-4VP) was prepared by the sequential anionic addition, with *n*-butyllithium (*n*-BuLi) (Aldrich) as an initiator, in tetrahydrofuran (THF) (Aldrich) at −68 °C under a nitrogen atmosphere.[20] Both the styrene (Aldrich) and 4VP (Aldrich) monomers were purified by drying over calcium hydride and distillation under vacuum three times before use. The *n*-BuLi was used as received, and its concentration was determined by titration. The exact amount of initiator needed for a specific molecular weight of PS was added first to the THF (which had been previously dried over potassium–benzophenone complex) and then distilled into polymerization flask. Styrene monomer was added dropwise with additional THF to the stirred mixture in the reaction flask, and enough diphenylethylene was subsequently added to cap the polystyrene living ends. A portion of the solution containing capped polystyrene was removed for characterization of the PS block. A calculated amount of 4VP was then added slowly, and a portion of the solution containing the desired VP chain length (240) of poly(S-b-4VP) was removed. The polymer precipitated in 10-fold excess volume of rapidly stirred petroleum ether (except that PS was precipitated in methanol) and dried in a vacuum oven at 70 °C for several days. The PS used in this system has a polydispersity of 1.30 and a molecular weight of ~27 500; both determined by GPC (Varian). The VP content was characterized by NMR (Varian, XL200) based on the peak area ratio of the pyridine-to-styrene resonances, and the result (240 VP) was in agreement with the expected composition and was further confirmed by titrating the polymer in chlorobenzene with perchloric acid.

Quaternization of PVP Blocks. The poly(S-b-4VP) was quaternized by adding 20-fold molar excess of freshly distilled decyliodide to a 3% THF solution of the previously dried polymer and refluxing the mixture under nitrogen for several days. The resulting solution was concentrated to about 5% of the initial volume by rotary evaporation. The polymer was recovered by precipitation into a 20-fold excess volume of hexane (Aldrich). After filtration, the quaternized product was dried in a vacuum oven at 70 °C to remove residual solvent. The completion of quaternization was determined by infrared spectroscopy via the disappearance of the pyridine adsorption at 1414 cm^{-1}.

Spreading of Polymer Films. The 4:1 chloroform/isopropyl alcohol mixed solvent was used as a spreading solvent. Polymer was kept in a desiccator and redried in a vacuum oven at 70 °C for 24 h before use. Chloroform (Aldrich) and isopropyl alcohol (Aldrich, HPLC grade) were freshly dried and distilled over P_2O_5 and CaO, respectively. The 0.5 mg/mL polymer stock solutions were prepared with the mixed solvent. In all measurements a 0.1-mL solution was deposited dropwise (18–20 drops) from a Hamilton gastight syringe onto the pure water surface, and 15 min was allowed for solvent evaporation before compression of the surface film was initiated.

Pressure-Area (π-A) Measurement of the Polymer Films. The surface pressure and area were measured on a LAUDA Model D Langmuir film balance. The total surface area of the trough is 927 cm^2, and the volume of the subphase water is 1.3 L. The water subphase was purified and deionized with a Millipore Milli-Q system (18 MΩ resistivity) equipped with an organic residue cartridge, and the temperature of the subphase water was maintained constant by a thermal circulator (Lauda). The compression rate was 15.4 mm/min, and the resolution of the surface pressure measurement is 0.1 mN/m. Several symbols are used to identify particular points of the isotherms. The area/molecule at which $\pi > 0$ is labeled A_{on}, the area/molecule at which a phase transition is observed is A_t, and the surface pressure associated with a first-order transition is termed π_t. The limiting area per molecule, A_{lim}, is determined from the intersection of the plateau extrapolation and the extrapolation of the steeply rising portion of the isotherm at high π.

Transmission Electron Microscope Observation of the Polymer Films (TEM). The polymer films were transferred from the water surface onto the EM grid by the Langmuir–Blodgett (LB) technique[21,22] as modified by Fischer and Sackmann. First, a sandwich-type package was made which consists of (i) a plastic coverslip to support the whole system, (ii) a layer of Formvar for attaching the EM grid onto the coverslip, and (iii) a layer of evaporated carbon which renders the surface conductive. Such an assembly can provide a large area which eliminates edge effects during the procedure of transferring a monolayer from a water surface onto the EM grid. The assembled package was clipped to a lifting rod which moves vertically with respect to the water surface at a constant rate. The coverslip containing the EM grid was submerged in the water phase prior to the spreading of the polymer solution. Once the film was spread and the desired transferring surface pressure reached, the EM grid assembly was lifted upwards toward the water surface at a constant speed (1 mm/min), while the surface pressure was kept constant. We have ob-

(4) Gaines, G. J., Jr. *Insoluble Monolayers at Liquid-Gas Interfaces*; Interscience: New York, 1966.
(5) Sauer, B. B.; Yu, H.; Tien, C.-F.; Hager, D. F. *Macromolecules* **1987**, *20*, 393.
(6) Sauer, B. B.; Yu, H.; Kim, M. W. *Langmuir* **1989**, *5*, 278.
(7) Lee, E. M.; Thomas, R. K.; Penfold, J.; Ward, R. C. *J. Phys. Chem.* **1989**, *93*, 381.
(8) Bringuier, E.; Vilanove, R.; Gallot, Y.; Selb, J.; Rondelez, F. *J. Colloid Interface Sci.* **1985**, *104*, 95.
(9) Niwa, M.; Hayashi, T.; Higashi, N. *Langmuir* **1990**, *6*, 263.
(10) Granick, S.; Herz, J. *Macromolecules* **1985**, *18*, 460.
(11) Reference 6 and references therein.
(12) Niwa, M.; Higashi, N. *Macromolecules* **1989**, *22*, 1000.
(13) Fuhrhop, J.-H.; Fritsch, D. *Acc. Chem. Res.* **1986**, *19*, 130.
(14) Wollman, D.; Williams, C. E.; Eisenberg, A. *J. Polym. Sci. Phys.*, in press.
(15) Price, C. In *Developments in Block Copolymers—1*; Goodman, I., Ed.; Elsevier: Applied Science: London, 1982; Chapter 2.
(16) (a) Selb, J.; Gallot, Y. In *Developments in Block Copolymers—2*; Goodman, I., Ed.; Elsevier Applied Science: London, 1985; Chapter 2. (b) Desjardins, A.; Gouin, J.-P.; van de Ven, T. G. M.; Williams, C. E.; Eisenberg, A. Presented at 33rd International Symposium on Macromolecules; Montreal, July 1990, Session 2.5.5.
(17) *Encyclopedia of Polymer Science and Engineering*; Kroschwitz, J. I., Ed.; Wiley-Interscience: New York, 1985; Vol. 2.
(18) Gouin, J.-P.; Williams, C. E.; Eisenberg, A. *Macromolecules* **1989**, *22*, 4573.
(19) Feng, D.; Wilkes, G. L.; Leir, C. M.; Stark, J. E. *J. Macromol. Sci.-Chem.* **1989**, *A26(8)*, 1151.
(20) Gauthier, S.; Eisenberg, A. *Macromolecules* **1987**, *20*, 760.
(21) Fischer, A.; Sackmann, E. *Nature* **1985**, *313*, 299.
(22) Neuman, R. D.; Fereshtehkhou, S. *J. Colloid Interface Sci.* **1988**, *125*, 34.

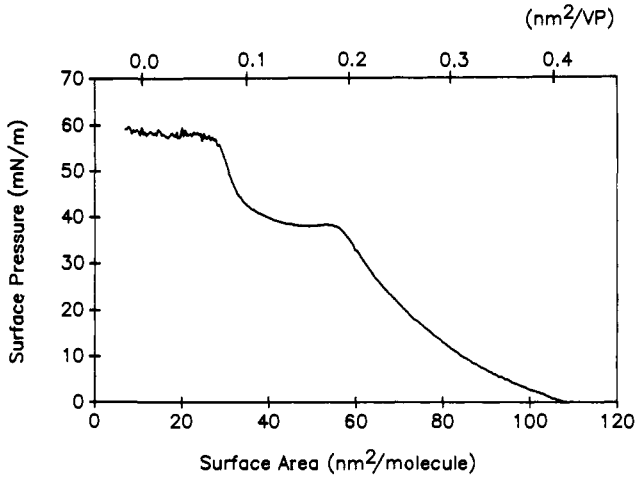

Figure 1. Surface pressure vs area per molecule (and area per VP residue) at 25 °C for a film of **1** at the air–water interface.

served from TEM photographs that no apparent structural defects in the transferred monolayers arise if the lifting rate is kept below 5 mm/min. Finally, the grids with transferred films were shadowed with gold/palladium (60/40) in a Philips E600 series vacuum coater at a shadowing angle of 15–25°. Each EM grid was organized with its dipping direction either parallel or perpendicular to the shadowing direction. The TEM image was observed by a JOEL-CX100-TEMSCAN analytical transmission electron microscope under 100 kv. Features in the electron photomicrographs with this procedure are highly reproducible over the entire surface.[23]

Results and Discussion

The π-A isotherm at 25 °C for

$$(PS)_{260}(\text{dec-4-PVP}^+\text{I}^-)_{240}$$
1

is shown in Figure 1. Several features are of interest in this isotherm. The area value, A_{on}, at which surface pressure is first discernible (+0.1 mN/m above baseline) appears to be large overall (109 nm^2/molecule) but is in fact relatively small when considered per VP residue. The area per VP residue can be estimated by subtracting the area contribution of the hydrophobic, surface-adsorbed PS block. By using an experimentally derived expression for the interfacial area of a PS block,[24] a value of 10.8 nm^2/PS block can be calculated. The A_{on} in terms of A/VP residue is thus ~0.41 nm^2/VP. The onset of surface pressure occurs abruptly compared with that observed by Kawaguchi and co-workers[25] for short (<70 VP residues) alkylated (R = C_8, C_{12}) 4-VP homopolymers. Further compression of the block polyelectrolyte leads to a film which is rather incompressible, and at 57 nm^2/molecule (0.19 nm^2/VP) a discontinuity indicative of a phase transition occurs at $A = A_t$. Further compression leads to a highly compressible region and an almost flat, first-order-like isotherm. At ~36 nm^2/molecule (0.11 nm^2/VP), the film becomes relatively incompressible once again, and π increases sharply until a possible film collapse/rearrangement occurs at 28 nm^2/molecule (0.07 nm^2/VP residue).

An understanding of the relationship between the isotherm properties, molecular orientations, and monomer conformations can be speculated upon on the basis of earlier work on polymer monolayers.[1-6,8-12,26] It is important to note that much of the interesting isotherm behavior in Figure 1 is occurring in a highly concentrated surface regime. Both the onset of the (apparent) first-order phase transition (0.19 nm^2/VP) and the film's limiting area (A_{lim} = 0.11 nm^2/VP) occur at areas considerably less than the area of an alkylated 4-VP residue lying flat on the surface (~0.48 nm^2, estimated from molecular models) with its alkyl chain perpendicular to the surface. Evidently the molecular orientations probed by Figure 1 involve some three-dimensional conformations of the vinylpyridinium chain.

Transmission electron micrographs (TEMs) of LB films deposited isobarically at low, intermediate, and plateau surface pressures greatly aid in an analysis of the structures of these films (Figure 2). The TEM of a film deposited at low π (Figure 2a) exhibits a relatively regular structure—a series of "cores" ~34 nm in diameter separated by distances (center-to-center) of ~125 nm.[27] The height of the core estimated from shadowing is ~8 nm. A film deposited along the rising portion of the isotherm (15 mN/m, Figure 2b) retains the same structural features as observed in Figure 2a (core of ~30 nm diameter, core height of ~8 nm) but has a considerably reduced average core–core distance (~90 nm). The electron micrograph (Figure 2c) of the film deposited from the plateau also retains the structural features of the core, but the core–core distance is reduced to ~45 nm. There is also evidence for coalescence of micelles.

What is the relationship between the isotherms of $(PS)_{260}$-$(\text{dec-4-PVP}^+\text{I}^-)_{240}$ and the aggregates visualized in the Langmuir–Blodgett TEMs? The aggregates appear to be *surface micelles* because of their dimensional similarity and are composed of a central region of PS blocks (the "core") and a corona of highly extended dec-4-PVP$^+$I$^-$ chains. Examining the film removed at low π (2 mN/m) it is seen that the core-to-core edge distance (~91 nm) is on the order of twice the length of two extended PVP chains. The onset of surface pressure at A_{on} (109 nm^2/molecule, ~0.41 nm^2/VP) is thus associated with PVP chains from adjacent micelles interacting with one another. The value of A_{on} is about 20% less than that expected for the sum of an adsorbed PS_{260} block (10.8 nm^2)[24] and an alkylated PVP chain whose alkyl groups extend into the air phase. For two reasons, these data are consistent with π arising at A_{on} from the interaction of *self-assembled* unimers rather than unimers oriented isotropically on the surface. Firstly, assembled unimers will have considerably less free surface area than an array of nonoriented unimers and will thus exhibit smaller A_{on} values than nonoriented unimers. Secondly, the decyl side chains do not manifest themselves in the isotherm with measurable surface pressures (~1–2 mN/m) at large areas (1.0 nm^2 < A/VP < 10.0 nm^2). Finite surface pressures at such large areas, accompanied by first-order behavior, are anticipated on the basis of the extensive series of isotherms reported for alkylated 4-PVP homopolymers.[25] In these examples, a first-order transition evidently arose from the forcing of alkyl chains from a horizontal, surface adsorbed state to a vertical state. A complete absence of surface pressure in the A/VP > 0.50 nm^2 suggests that the decyl chains are in a vertical configuration *prior* to A_{on} being reached. This configuration arises because the PVP chains are so densely packed in the preassociated state that the alkyl chains are forced from the surface-adsorbed configuration to the vertical configuration. Estimates of the core dimension leads to an aggregation number of ~120 for each micelle.[27]

At higher surface concentrations (Figure 2b), the core–core distance is considerably reduced, and π has substantially increased. This is consistent with the interpenetration of PVP chains from adjacent micelles. At $\pi = \pi_t$, a phase transition occurs; the surface packing picture (Figure 2c) looks much like a series of PS cores in close proximity with the entire surface being occupied by PS and dec-4-PVP. For small molecular weight amphiphiles[28] a first-order phase transition is frequently observed in the liquid

(23) We have also recently established that LB films of **1** deposited on mica and glass surfaces retain the features and dimensions described herein; these LB films were however visualized with atomic force microscopy and will be reported elsewhere.

(24) Kumaki, J. *Macromolecules* **1988**, *21*, 749.

(25) Kawaguchi, M.; Itoh, S.; Takahashi, A. *Macromolecules* **1987**, *20*, 1052.

(26) Kawaguchi, T.; Nakahara, H.; Fukoda, K. *Thin Solid Films* **1989**, *155*, 29.

(27) Zhu, J.; Eisenberg, A.; Lennox, R. B. *Langmuir*, in press. Five independent methodologies for determining the aggregation number N of micelles observed in LB films (PS_{260}(dec-4-PVP$^+$I$^-$)$_{240}$) have been described, each based on an examination of TEMs. These determinations represent a yield of N ranging from 83 ± 28 to 146 ± 58, with the greatest confidence placed on a method (individual micelle area method) which yields an N = 131 ± 35.

(28) (a) Bell, G. M.; Combs, L. L.; Dunne, L. J. *Chem. Rev.* **1981**, *81*, 15. (b) Cadenhead, D. A.; Müller-Landau, F.; Kellner, B. M. J. In *Ordering in Two Dimensions*; Sinha, S. K., Ed.; Elsevier: North Holland, 1980.

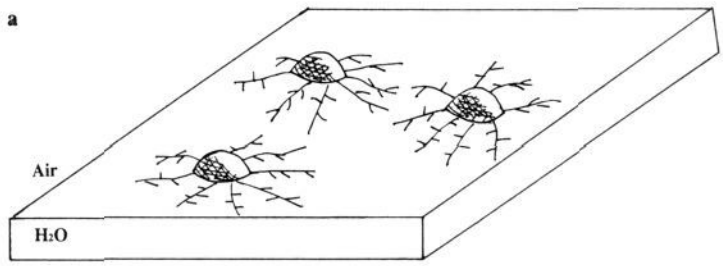

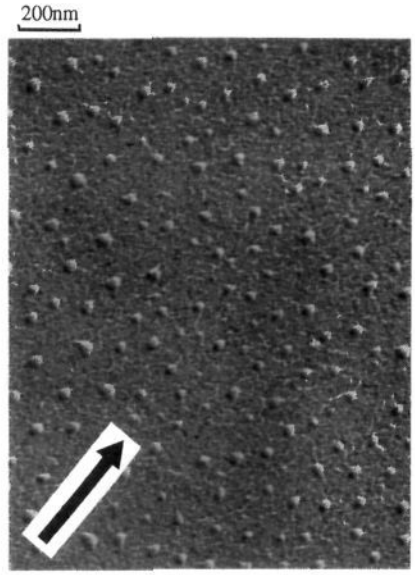

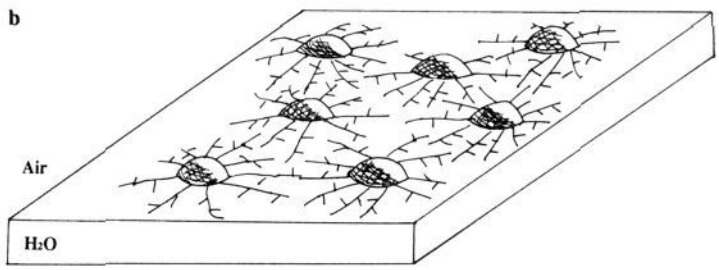

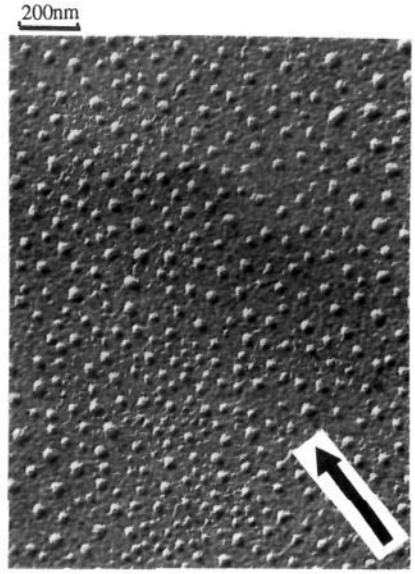

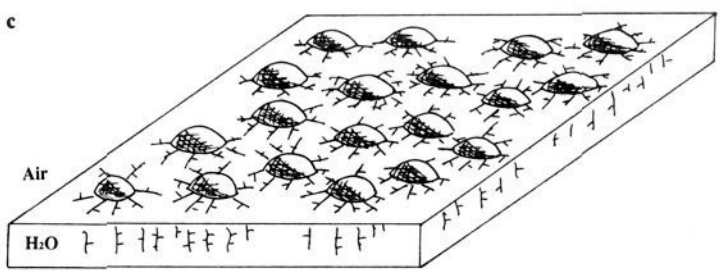

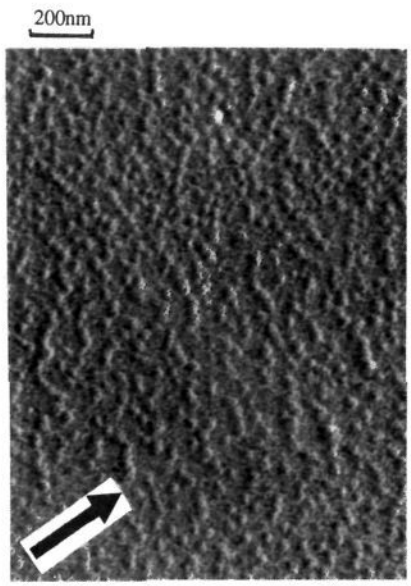

Figure 2. (a) Transmission electron micrographs of an LB film of **1** deposited at 2 mN/m and 25 °C. Arrow indicates direction of shadowing. Calibrant bar represents 200 nm. (b) As per (a) except deposition was performed at 15 mN/m. (c) As per (a) except deposition was performed at the plateau pressure. Beside each electron micrograph is a schematic representation of the surface film formed at the air/water interface and how it relates to the micrographs. Although represented as a solubilization process which starts at the terminal VP and works toward the polystyrene block, an alternative process where solubilized VP "loops" and surface-adsorbed VP "trains" coexist is also very possible.

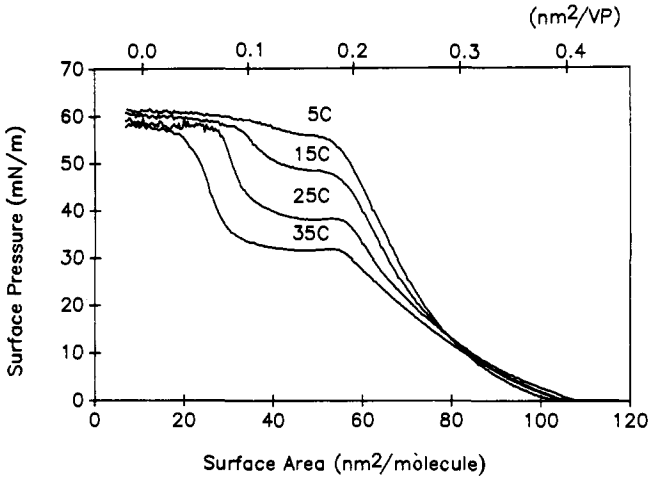

Figure 3. Series of surface pressure/area isotherms of **1** at indicated temperatures.

state of the film and is often ascribed to an LE (liquid expanded) → LC (liquid condensed) process. For simple amphiphiles the first-order transition mechanism can be viewed schematically as an incremental change in orientation of alkyl chains from a horizontal, water adsorbed state to a vertical, air-solubilized state. This however is not a realistic mechanism for the polyelectrolyte of 240 residues described in this work. The mechanism which we favor[29] involves the incremental solubilization of decylated VP residues into the aqueous subphase as the surface area is steadily reduced by the moving barrier. This mechanism is akin to Langmuir's proposal of pressure-induced solubilization of components of protein films.[30] The electron micrograph in Figure 2c is consistent with the PS "core" of the surface micelle resting atop the partially submerged ionic chains. The aggregate morphology observed in Figure 2 and attribution of the plateau region in the isotherm to incremental solubilization of the alkylated polyelectrolyte chains leads us to term this a "starfish ↔ jellyfish" transition for illustrative purposes.

The temperature dependence of the surface pressure properties of **1** provides insight into the nature of the surface-adsorbed film and the molecular details of the phase transition (Figure 3). Notable in a general sense is the observation that the plateau pressure (π_t) and A_{lim} decrease with increasing temperature. The π_t behavior (a temperature "inversion") is rather unusual in that it often implies, upon analysis, that the phase transition accompanying an LE → LC process (ostensibly a disorder → order transition) is accompanied by a *positive* ΔS. Similar observations have been observed for other polymer films,[31-33] but the provenance of positive ΔS values is not evident in all cases. Application of the corrected form[31,34,35] of the Clapeyron equation

$$\Delta H = T\Delta A(d\pi/dT - d\gamma^\circ/dT) = T\Delta S \qquad (1)$$

where ΔA is the area change of the transition (−0.090 nm²/VP residue), and data from Figure 3 lead to a ΔH = +2.3 kcal/mol of VP residues at 25 °C and ΔS = +7.6 eu. A $\Delta S_{trans} > 0$ is consistent with the "starfish ↔ jellyfish" transition, where the surface-localized radial micelle (starfish) is in a low entropy, 2D, surface-confined state. Compression, causing the surface-adsorbed decylated PVP^+ chain to be driven into the subphase, results in a considerable increase in chain-associated entropy as the chains now occupy a quasi-2D space rather than a 2D space. The A_{lim} effect, on the other hand, suggests that chain submersion is strongly temperature dependent and that at low T (i.e., 5 °C) substantially fewer VP residues are submerged than at high T (i.e., 35 °C). The "starfish ↔ jellyfish" transition therefore appears to be incomplete at low T's, and the incompressible state at high π corresponds to compression of "incomplete jellyfish". This incompressibility probably originates from a combination of short range polyelectrolyte–polyelectrolyte interactions, volume packing restrictions, and the solubility limitations alluded to above. The π_t and A_{lim} temperature dependences are therefore consistent with the analysis of both the 25 °C isotherm and the LB film electron micrographs.

The driving force for the formation of the 2D micelle is apparently a delicate balance between hydrophobic and hydrophilic factors. The ionic PVP chain is strongly surface-adsorbed at low π because of its decyl comb side groups. Polystyrene blocks are strongly hydrophobic and evidently aggregate so as to reduce PS/water interactions. The balance between the interfacial energies of all the component groups, van der Waals attractive forces, electrostatic repulsive forces, and geometric packing requirements lead to a low-energy configuration as a radial micelle-like aggregate. A quantification of the factors controlling both the surface aggregate morphology and the phase transition is currently under investigation in our labs with a number of structural variants of **1**; these studies will be reported shortly.

The phenomenon of amphiphile self-association had been suggested by Langmuir in 1933[36] for fatty acids and alkyl phenols and has been reported for several systems in regards to domains in the LE/LC phase transition. Evidence has been lacking however for the existence of thermodynamically controlled aggregates of uniform size and hence uniform aggregation number (i.e., micelles) at the air–water interface. Surface aggregation in arachidic acid at π = 0 has been observed;[37] the morphology of this self-assembled state is complex however and may arise from LB artefacts.[22]

The existence of highly regular and ordered surface micelles at both the air–water interface and in deposited LB films is of interest from both fundamental and applied points of view. From a basic standpoint, the isotherms as presented in this work will provide considerable information (at subnanometer resolution) concerning the energetics of the entire process of micelle–micelle interactions (long and short range), micelle–micelle coalescence phenomena, and micellar phase transitions. The two-dimensional (or quasi-2D) nature of these phenomena in this system provides considerable simplification compared to the three-dimensional micelle situation. From a practical perspective we have shown that these aggregates are stable and can be deposited on a solid substrate as monomolecular polymer films. Viewed as an assembly of micelles, at low surface pressures the surface density is ~10 G particles/cm². It is likely that once formed, the surface aggregates are kinetically stable and therefore unimer–micelle exchange is probably very slow. The control of monomolecular film morphology via the choice of deposition π offers interesting possibilities regarding the modification of the surface of a solid substrate with block polyelectrolytes. These and other aspects of this system are currently under active investigation in our laboratories.

Summary

The results presented here, concerning the monomolecular films formed from a PS-decPVP⁺I⁻ block polyelectrolyte provide new insights into the interfacial behavior of amphiphilic polymers. Novel surface micellization phenomena of the AB block ionomer is evident from electron micrographs of LB films, their correlations

(29) Other possible mechanisms include a flat ↔ edge-on conformational change in the VP rings or a coalescence of the circular aggregates. Neither of these processes is fully consistent with both the isotherm data and the electron microscopy information.

(30) Langmuir, I.; Waugh, D. F. *J. Am. Chem. Soc.* **1940**, *62*, 2771.
(31) Biegajski, J. E.; Cadenhead, D. A.; Prasad, P. N. *Langmuir* **1988**, *4*, 689.
(32) Duda, G.; Schouten, A. J.; Arndt, T.; Lieser, G.; Schmidt, G. F.; Bubeck, C.; Wegner, G. *Thin Solid Films* **1988**, *159*, 221 and references therein.
(33) Fox, H. W.; Taylor, P. W.; Zisman, W. A. *Ind. Eng. Chem.* **1947**, *39*, 1401.
(34) Adamson, A. W. *Physical Chemistry of Surfaces*, 3rd ed.; J. Wiley and Sons: Toronto, Ontario, Canada, 1976.
(35) Motomura, K. *Adv. Colloid Interface Sci.* **1980**, *12*, 1.
(36) Langmuir, I. *J. Chem. Phys.* **1933**, *1*, 756.
(37) (a) Fischer, A.; Sackmann, E. *J. Colloid Interface Sci.* **1986**, *112*, 1. (b) Lösche, M.; Sackmann, E.; Möhwald, H. *Ber. Bunsenges Phys. Chem.* **1984**, *87*, 848.

with the features of π/A isotherms, and with the temperature dependence of the isotherms. An unusual surface phase transition is observed for this material, where $\Delta S_{trans} > 0$; a model of this process has been presented ("starfish ↔ jellyfish" transition) and involves the transformation of 2D radial surface micelles into quasi-2D aggregates with the poorly water-soluble polyelectrolyte chains being submerged in the aqueous subphase.

Acknowledgment. We thank NSERC Canada (R.B.L., A.E.), the U.S. Army Research Office (J.Z., A.E.), and the McGill Graduate Faculty (R.B.L.) for financial support of this research. R.B.L. thanks D. A. Cadenhead for helpful discussions, and we thank M. Harrigan, McGill Department of Occupational Health, for providing us with assistance with the electron microscope experiments.

Scanning Tunneling Microscopy Studies of Carbon–Oxygen Reactions on Highly Oriented Pyrolytic Graphite

Hsiangpin Chang† and Allen J. Bard*

Contribution from the Department of Chemistry, The University of Texas at Austin, Austin, Texas 78712. *Received February 26, 1991*

Abstract: The oxidation of highly oriented pyrolytic graphite (HOPG) in air at elevated temperatures was studied by examination of the oxidized HOPG by scanning tunneling microscopy (STM). Etch pits of uniform size and monolayer depth were readily formed on preexisting defects or generated vacancies in the HOPG basal plane by heating freshly cleaved HOPG samples in air at 650 °C. The density of the pits in different samples of HOPG varied from 0.1 to 13 μm^{-2}. When the oxidized HOPG samples were reheated and reexamined by STM, the original etch pits had grown and new, smaller etch pits were found. Therefore, pit growth initiation occurred during each cooling–reheating cycle, and consecutive heating cycles could control the pit density. At higher temperatures, above 700 °C, carbon abstraction occurred on the basal plane of graphite, which generated additional vacancies and initiated new etch pits continuously throughout the period of heating at this temperature. The rates of carbon abstraction in both cases depended on the vacancy-density of the HOPG. On HOPG samples treated with different materials, both those expected to be chemically active (e.g., $FeCl_3$, CdS, H_2PtCl_6) or inert (e.g., NaCl, Al_2O_3), numerous etch channels were found on the surfaces after oxidation, representing the paths of randomly moving particles. Because similar channels are formed with all of these materials, these channels are probably mainly produced by mechanical interactions by the particles on the graphite surface.

Introduction

Recently we reported the formation of monolayer etch pits on HOPG by gasification reactions with dioxygen as imaged and studied by STM.[1] These etch pits were reproducibly formed across the entire surface of a freshly cleaved HOPG sample, and their size (5–400 nm) increased linearly with reaction time. Several applications of these etch pits were proposed. For example, they could be useful as markers and molecular containers for STM imaging, and may behave as active sites of controlled density for chemical and electrochemical reactions. We report here more detailed STM studies of the oxidation (gasification) of HOPG in air, including studies in which various species were added to the HOPG surface. Such studies provide some insight into the early stages of graphite gasification. Moreover, we felt that a better understanding of the factors that govern formation of the etch pits would lead to better control of their shape, size, and density.

There have been extensive studies of gasification reactions of carbon, especially graphite, in pioneering work by Hennig, Thomas, Yang, and others[2-5] using microscopic techniques, including optical microscopy, scanning electron microscopy (SEM), and etch-decoration transmission electron microscopy (ED-TEM). A particular advantage of microscopic studies of graphite oxidation, compared, for example, to weight loss or product yield measurements, is that it is possible, in favorable circumstances, to distinguish sites of different reactivity on the carbon surface.[2c] It is clear that carbon surfaces (and probably the surfaces of most other substances) are heterogeneous and that, in many cases, reactions occur at much higher rates at certain sites, e.g., lattice defects or impurity sites. Microscopic methods in general, and as we show here, STM in particular can provide information about site reactivity in carbon gasification, which is of interest in connection with many important processes, e.g., combustion and water gas production.[3] A great deal of information has been obtained, including surface images with near atomic resolution, with ED-TEM,[2,4,5] invented by Henning and later used by Thomas, Yang, and others. The mechanism of the C–O_2 reaction is temperature-dependent. At temperatures below 700 °C, the carbon–oxygen reaction is highly dependent on the nature of the carbon sites on the HOPG; oxidation is initiated mainly at defects, vacancies, or edge atoms along cleavage steps, presumably because of their unoccupied sp^2 orbitals. At temperatures above 700 °C,

† Current address: Westhollow Research Center, Shell Development Co., Houston, TX 77082.

(1) Chang, H.; Bard, A. J. *J. Am. Chem. Soc.* **1990**, *112*, 4598.

(2) (a) Yang, R. T. In *Chemistry and Physics of Carbon*; Walker, P. L., Jr., Thrower, P. A., Eds.; Marcel Dekker: New York, 1984; Vol. 19, pp 163–210. (b) Hennig, G. R. *Ibid.*; Walker, P. L., Ed.; 1966; Vol. 2, pp 1–50. (c) Thomas, J. M. *Ibid.*; Walker, P. L., Ed.; Marcel Dekker: New York, 1965, Vol. 1, pp 121–203. (d) Walker, R. T. K. *Catal. Rev.-Sci. Eng.* **1979**, *19*, 161.

(3) (a) Kinoshita, K. *Carbon: Electrochemical and Physical Properties*; Wiley: New York, 1988; Chapter 4. (b) Strange, J. F.; Walker, P. L., Jr. *Carbon* **1976**, *14*, 345. (c) Rodriguez-Reinoso, F.; Thrower, P. A. *Ibid.* **1974**, *12*, 269. (d) KcKee, D. W. *Ibid.* **1970**, *8*, 623. (f) Laine, N. R.; Vastola, F. J.; Walker, P. L. *J. Phys. Chem.* **1963**, *67*, 2030. (e) Bonner, F.; Turkevich, J. *J. Am. Chem. Soc.* **1951**, *73*, 561. (f) Lewis, W. K.; Gilliland, E. R.; McBride, G. T., Jr. *Ind. Eng. Chem.* **1949**, *41*, 1213.

(4) (a) Yang, K. L.; Yang, R. T. *AIChE J.* **1985**, *31*, 1313. (b) Yang, R. T.; Yang, K. L. *Carbon* **1985**, *23*, 537. (c) Duan, R.-Z.; Yang, R. T. *Chem. Eng. Sci.* **1984**, *39*, 795. (d) Yang, R. T.; Wong, C. *J. Catal.* **1984**, *85*, 154. (e) Yang, R. T.; Wong, C. *Science* **1981**, *214*, 437. (f) Yang, R. T.; Wong, C. *AIChE J.* **1983**, *29*, 338. (g) Wong, C.; Yang, R. T.; Halpern, B. L. *J. Chem. Phys.* **1983**, *78*, 3325. (h) Wang, R. T.; Wong, C. *Ind. Eng. Chem. Fundam.* **1983**, *22*, 380. (i) Yang, R. T.; Wong, C. *Rev. Sci. Instrum.* **1982**, *53*, 1488. (j) Yang, R. T.; Wong, C. *J. Chem. Phys.* **1981**, *75*, 4471. (k) Wong, C. Ph.D. Thesis, SUNY-Buffalo, Amherst, NY, 1983. (l) Cen, P.; Yang, R. T. *Carbon* **1984**, *22*, 186.

(5) (a) Hennig, G. R. *J. Chem. Phys.* **1964**, *40*, 2877. (b) Hennig, G. R. *J. Inorg. Nucl. Chem.* **1962**, *24*, 1129. (c) Evans, E. L.; Griffiths, R. J. M.; Thomas, J. M. *Science* **1970**, *171*, 174. (d) Feates, F. S. *Trans. Faraday Soc.* **1968**, *64*, 3093. (e) Montet, G. L.; Myers, G. E. *Carbon* **1968**, *6*, 627.

0002-7863/91/1513-5588$02.50/0